

Contact Stress Analysis of the Conforming Post-Cam Mechanism in Posterior-Stabilized Total Knee Arthroplasty

Yukio Akasaki, MD,* Shuichi Matsuda, MD, PhD,* Takeshi Shimoto, PhD,†
Hiromasa Miura, MD, PhD,* Hidehiko Higaki, PhD,† and Yukihide Iwamoto, MD, PhD*

Abstract: The present study evaluated the effects of extent of conformity of post-cam design on contact area and stress at post-cam mechanism using 4 different posterior-stabilized prostheses. TRAC and Alpina with full-conformed post-cams exhibited the largest contact area at 90° and 120°. PFC sigma RPF with partial conformed post-cam had the largest contact area at 150°. Scorpio NRG with less conformed post-cam had smaller contact area than the others. Lifting of femoral component decreased contact area and increased contact stress of TRAC and Alpina. Recent modifications of post-cam design have increased contact area, contributing to lower contact stress. None of these prostheses exhibited constant low contact stress throughout flexion. Further modifications of post-cam mechanism are necessary to provide lower contact stress throughout deep knee flexion. **Key words:** post-cam, posterior-stabilized, conformity, contact stress, total knee arthroplasty, polyethylene.

© 2008 Elsevier Inc. All rights reserved.

Since its introduction in the mid 1970s [1], posterior-stabilized total knee arthroplasty (PS-TKA) has been widely used for patients requiring primary and revision TKA. Long-term follow-up studies have reported satisfactory results [2,3]. The complications of the post-cam mechanism, however, including dislocation of the knee and fracture or severe wear of the post were reported [4-9]. In some retrieval analyses, post damages were found both anteriorly and posteriorly involved in hyperextension and hyperflexion respectively.

Surgical techniques and rehabilitation programs have been improved to achieve a greater range of movement than 130° to meet the needs of patients who perform deep knee flexions, such as squatting and kneeling, as part of their daily activities [10]. The design of TKA should be modified to achieve the endurance of prosthesis even with deep knee flexion.

A number of biomechanical studies have demonstrated the generation of a high anteroposterior shear force at the tibiofemoral joint during deep knee flexion [11-16]. In our previous study [17], very high contact stress was applied to the post-cam interface, revealing that the shape and apical orientation of the cam affects contact stress significantly. It is reported that high contact stress results in the increasing amount of polyethylene wear in knee wear simulator [18,19]. Therefore, low contact stress is one of the major factors that contribute to prevent polyethylene wear [20-22]. A large contact area and high conformity of the post-cam interface would be necessary to reduce wear problems. Recently, many of post-cam designs have

*From the *Department of Orthopaedic Surgery, Graduate School of Medical Sciences, Kyushu University, Fukuoka, Japan; and †Department of Mechanical Engineering, Kyushu Sangyo University, Fukuoka, Japan.*

Submitted December 26, 2006; accepted May 18, 2007.

No benefits or funds were received in support of the study.

Reprint requests: Shuichi Matsuda, MD, PhD, Department of Orthopaedic Surgery, Graduate School of Medical Sciences, Kyushu University, 3-1-1 Maidashi, Higashi-ku, Fukuoka, 812-8582, Japan.

© 2008 Elsevier Inc. All rights reserved.

0883-5403/08/2305-0015\$34.00/0

doi:10.1016/j.arth.2007.05.023

been modified to contain a larger contact area. It is important to analyze the effects of the conforming post-cam mechanism on the contact stress generated under anteroposterior force with and without lift-off motion, which occurs in deep knee flexion after PS-TKA and causes eccentric loading and premature wear of polyethylene. Many kinematic analyses have demonstrated high and uneven loading applied to the tibiofemoral articular surface with condylar lift-off during knee bending [23-26]. Therefore, primarily, the tibiofemoral articular surface has been modified to reduce edge loading during deep knee flexion. However, the effect of condylar lift-off on contact characteristics of post-cam mechanism should also be evaluated.

This study was designed to evaluate the effects of the extent of the conformity of the post-cam design on the contact area, stress, and location at the post and cam mechanism of PS-TKA, with or without lift-off motion. Four different prosthesis designs were compared. We hypothesized that design characteristics would affect the contact area and stress at each angle of flexion, and lift-off motion alters the loading pattern of each post-cam design. A post-cam interface with a higher degree of conformity could reduce the contact stress of the post-cam mechanism.

Materials and Methods

We analyzed the TRAC (Biomet, Warsaw, Ind; size 60 femoral component, size 60 tibial component), the Alpina (Biomet; size 5 femoral component, size 5 tibial component), the PFC sigma RPF (Depuy, Raynham, Mass; size 2 femoral component, size 2 tibial component), and the Scorpio NRG (Stryker, Allendale, NJ; size 7 femoral component, size 5 tibial component) PS-TKAs (Figs. 1-4 respectively). Design feature and size variation are shown in Tables 1 and 2. The experimental method we reported previously [17] was used in the present study. The femoral components were attached to a fixture that provided a flexion range of 90°, 120°, or 150°. The tibial component was implanted into a block of metal in the neutral position. The femoral and tibial fixtures were then mounted into a parallel-link 6-axis actuator.

A compressive posterior load of 500 N was applied to the tibial component against the femoral component parallel to the tibial base plate. The applied load of 500 N was determined according to the biomechanical study of Nagura et al [15]. The position of the femoral component in the sagittal plane was



Fig. 1. The TRAC prosthesis. This unit has a fully conforming post-cam mechanism.

adjusted until both the medial and lateral femoral condyles contacted the tibial articular surfaces. A digital electronic stress sensor (K-Scan sensor, Tekscan Inc, Boston, Mass) was used to detect contact areas and measure contact stresses, placed at the post-cam interface. The sensor has 2 separate sensing areas; each one is 33 × 28 mm and 0.1 mm thick and consists of 26 conductive rows and 22 columns whose intersection points form the sensing location. The device senses the location, timing, and pressure distribution of any contact 0 to 55 MPa with a coating material that varies its electrical resistance with force. An IBM desktop computer connected to the sensor recorded the stress at each intersection. The accuracy of this system has been previously evaluated [27-29]. Measurements were carried out at 90°, 120°, and 150° flexion using the TRAC, Alpina, PFC sigma RPF, and Scorpio NRG components. Measurements were performed 5 times for each component to permit calculation of the variance across the testing conditions. Peak contact stress, defined as the highest stress of all sensing locations, as well as the mean contact stress and contact area were calculated automatically by the Tekscan software. The center of contact area was



Fig. 2. The Alpina prosthesis. This device has a spherical-shaped post, whereas the post-cam mechanism conforms fully.

also determined. The distance from the deepest part of the tibial articular surface to the center of the contact area was defined as the contact location. Then, contact area and contact stress were measured again while lifting both medial and lateral femoral condyles 3 mm from the tibial articular surface at 120° of flexion using the TRAC, Alpina, PFC sigma RPF, and Scorpio NRG components.

The contact areas, mean and peak contact stresses, and contact locations were compared between the prostheses at each flexion angle; contact area and stresses with and without femoral condylar lift-off at 120° of flexion were also compared. Statistical significance was evaluated by analysis of variance and a post hoc Scheffe I test. Values of *P* less than .05 were regarded as significant.

Results

Contact Area

The TRAC and Alpina components exhibited the largest contact areas at 90° of 67.7 and 73.9 mm², respectively; these values were significantly larger

than those of the other prostheses (*P* < .001) (Fig. 5). The TRAC and Alpina units had decreased contact areas at 120° and 150°, although these components still had larger contact areas than the others at 120° (*P* < .001). The contact areas of the PFC sigma RPF increased with flexion, then the PFC sigma RPF had the largest contact area of all of the prostheses at 150° (81.6 mm²) (*P* < .001). The Scorpio NRG had smaller contact area than the other units. The Scorpio NRG showed the smallest contact area of all of the units at 120° (30.0 mm²) (*P* < .001), although displayed increased contact area at 150°.

Mean Contact Stress

Mean contact stress demonstrated an opposite trend as contact area. The TRAC and Alpina units had contact stresses at 90° of 6.7 and 7.3 Mpa, respectively, which were significantly lower than those of the other prostheses (*P* < .001) (Fig. 6). The TRAC and Alpina components exhibited increased contact stresses at 120° and 150°. These units still had lower contact stresses than the other units at



Fig. 3. The PFC sigma RPF prosthesis. The cam is in a distally apex shape, with a relatively flat surface from the posterodistal part to the posterior part.



Fig. 4. The Scorpio NRG prosthesis. The cam of this unit has oval shape and a relatively large radii of curvature posteriorly.

120° ($P < .001$). The PFC sigma RPF exhibited decreased contact stress with increasing flexion, displaying the lowest contact stress of all of the units (6.1 MPa) at 150° ($P < .001$). The Scorpio NRG demonstrated a similar stress pattern as the PFC sigma RPF, although the contact stresses were higher than the other prostheses at 120° (16.7 MPa) ($P < .001$).

Peak Contact Stress

The peak contact stress from 17 to 47 MPa was 2- to 3-fold as high as the mean contact stress at the same angle of flexion (Fig. 7). At 90° and 120°, the TRAC and Alpina components had the lowest contact stresses, measuring less than 18 MPa, which was significantly lower than those of the other units ($P < .001$). At 150°, the PFC sigma RPF exhibited the lowest contact stress of 19.8 MPa, which was significantly lower than those of the other prostheses ($P < .001$). The peak contact stress of the Scorpio NRG increased at 120° to the highest contact stress measured for all of the prostheses ($P < .001$); the stress measurement, however, decreased at 150°.

Contact Location

Significant differences were observed in the contact locations of each prosthesis at each angle of flexion (Fig. 8). The TRAC component exhibited the highest contact location at 90° and 150° ($P < .001$). At 90°, the contact location of the TRAC was 13.1 mm, moving to 14.2 and 14.6 mm at 120° and 150°, respectively. The contact location of the Alpina at both 90° and 120° was 9.7 mm, moving to 8.7 mm at 150°. The contact location of the Scorpio NRG peaked at midflexion, with measurements of 12.0, 15.1, and 13.1 mm at 90°, 120°, and 150°, respectively. In contrast, the contact location of the PFC sigma RPF bottomed at the midflexion, and this device possessed the lowest contact locations at all angles of flexion ($P < .001$). The contact location of the PFC sigma RPF was 7.1, 6.4, and 7.3 mm at 90°, 120°, and 150°, respectively.

Effect of Femoral Condylar Lift-Off

With a femoral condylar lift-off of 3 mm, the contact area of the TRAC decreased significantly from 61.3 to 44.2 mm², whereas the Alpina decreased from 58.7 to 36.5 mm² (Fig. 9). The mean and peak contact stresses of these components with lift-off exhibited significant increases from those of the original measured positions (Figs. 10 and 11). The Scorpio NRG demonstrated slight decrease in contact area and slight increase in the mean contact stress with lift-off (Figs. 9-11). The PFC sigma RPF unit did not show any significant changes in either contact area or stress.

Discussion

The post-cam mechanism plays one of the most important roles in knee flexion after PS-TKA, facilitating motions similar to normal knees, such as femoral rollback. Recently, complications of the post-cam mechanism, such as fracture, severe wear of the post, and dislocation of the knee have been reported [4-9]. In a retrieval analysis of 23 components that had been implanted for a mean of 35.6 months, Puloski et al [9] concluded

Table 1. Design Feature of the Prostheses

	TRAC	Alpina	PFC sigma RPF	Scorpio NRG
Design of the post	Round	Round	Curve	Curve
Design of the cam	Round	Round	Curve	Oval
Conformity	Full	Full	Partial	Partial

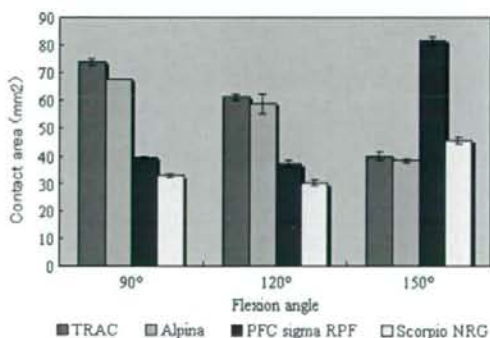
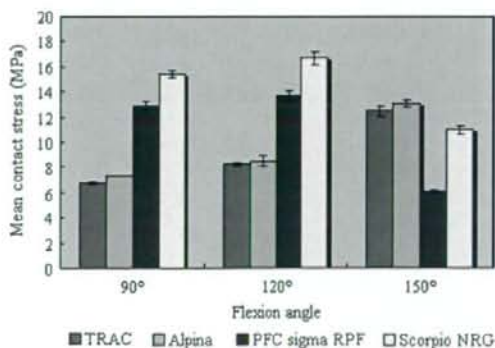
Table 2. Size Variation of the Prostheses

TRAC			Alpina			PFC sigma RPF			Scorpio NRG		
Size	Post height (mm)	Post width (mm)	Size	Post height (mm)	Post width (mm)	Size	Post height (mm)	Post width (mm)	Size	Post height (mm)	Post width (mm)
55	18.3	15.2	1	15	12	1	15.5	14.1	3	18.8	16.3
60	18.3	17.3	3	16	13	1.5	15.8	14.1	4	18.8	16.3
65	18.3	17.3	5	17	14	2	17.6	14.1	5	18.8	16.3
70	18.3	17.3	7	18	14.5	2.5	17.9	14.1	6	18.8	16.8
75	18.3	17.3	9	19	15	3	17.9	14.1	7	18.8	16.8
			11	20	16	4	21.7	16.3	8	18.8	16.8
			13	21	17				9	18.8	16.8

that the post-cam articulation could be an additional source of polyethylene wear debris. The variability in wear patterns observed among the different designs may be due to differences in the post-cam configuration. Mauerhan [6] reported 5 patients with fractures of the post causing subluxation of the femur. Of the 5 patients, 4 exhibited more than 130° flexion after PS-TKA; these patients could perform activities that involved kneeling and squatting. Although anteroposterior force on the tibiofemoral joint is not significantly increased during the gait cycle, biomechanical studies have demonstrated that the anteroposterior shear force at this joint is increased during deep knee flexion [11-16].

In this study, the 4 different post-cam designs exhibited significant differences in the contact area and contact stress at each flexion angle. The TRAC and Alpina had fully conforming surfaces in the sagittal plane (Figs. 1 and 2), displaying the same trend in contact area and contact stress with increasing angles of flexion. Although these devices showed the largest contact area and lowest contact stress from 90° to 120°, the contact area decreased significantly at 150°. The cams of both the TRAC and

Alpina units have round shapes with large radii of curvature; as the flexion angle increases, the cam partially loses contact with the post surface. These findings may suggest that the post-cam shape of the TRAC and Alpina components would exhibit better wear performance in daily activities, such as standing up from a chair or climbing up and down stairs, but are not suitable for squatting and kneeling activities that require greater than 120° of knee flexion. The post-cam mechanism of the PFC sigma RPF unit conformed partially in the sagittal plane (Fig. 3). This device increased contact area and decreased contact stress with increasing knee flexion, exhibiting the largest contact area and lowest contact stress at the 150° angle. The cam of the PFC sigma RPF is in a curved shape, with increasing radii of curvature from the distal part to the posterior part (Fig. 3), which results in almost full conformity between the post and cam at 150°. These findings suggest that the post-cam shape of the PFC sigma RPF components would be suitable for movements requiring 150° of knee flexion, such as squatting. The Scorpio NRG had less of conforming post-cam mechanism in the sagittal plane (Fig. 4). The cam of the Scorpio NRG has oval shapes with a

**Fig. 5.** Contact area (mm²) of each component.**Fig. 6.** Mean contact stress (MPa) of each component.

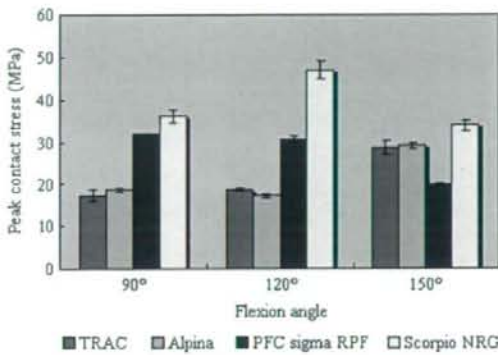


Fig. 7. Peak contact stress (MPa) of each component.

relatively large radii of curvature posteriorly. This design feature is congruent with the high values of contact stress in comparison to other prostheses. However, none of the prostheses examined exhibited constantly low contact stresses, the permissible compressive yield strength of UHMWPE (10 MPa) [30,31], throughout flexion.

Contact location is determined by multiple factors, including the shape of the cam, the position of cam attachment to the femoral component, and the curvature of the posterior femoral condyle. Higher contact point on the post is a risk factor of dislocation of the cam when abnormal motion occurs [23]. The contact location of the PFC sigma RPF remained lower than the other prosthesis throughout flexion, a feature that is beneficial for avoiding excessive stresses at the bone-implant interface and for preventing dislocation of the cam or fracture of the post. The total movements of the contact location during flexion for the TRAC, Alpina, and PFC sigma RPF devices were 1.5, 1.4, and 1.6 mm, respectively,

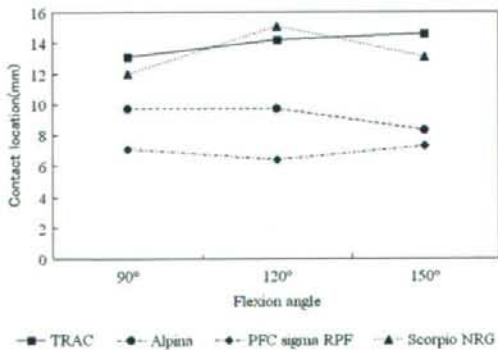


Fig. 8. Distance (mm) from the center of the contact area to the upper surface of the tibia.

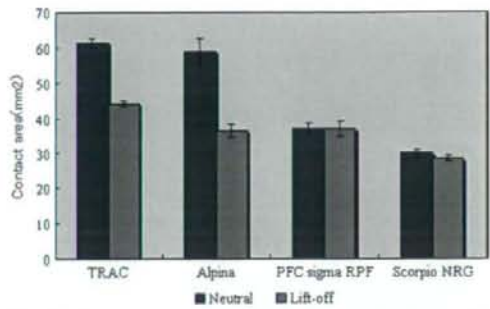


Fig. 9. Contact area (mm²) of each component with neutral and 3 mm lift-off of the femoral component at 120° of flexion.

which were smaller values than that of the Scorpio NRG (5.1 mm). The reduced movement of the contact location could be advantageous in preventing delamination of the polyethylene and in avoiding excessive wear. The concentration of contact stress in one spot, however, generates creep deformation, jeopardizing the longevity of the polyethylene [32,33]. It is necessary to consider both the sliding velocity and the contact stress when predicting polyethylene wear [34]. Therefore, it will be necessary to investigate the components under dynamic conditions to evaluate the effect of contact location on polyethylene wear.

The effect of femoral condylar lift-off on contact stress is also important in investigating the post-cam mechanism. Numerous kinematic analyses of the knee have demonstrated that the femoral condylar lift-off can occur during both normal gait and deep knee flexion [23-26]. Dennis et al [24] performed a fluoroscopic analysis of 20 patients after PS-TKA (PFC design; Johnson & Johnson, Raynham, Mass), revealing that femoral condylar lift-off was observed at some increment of knee flexion in 80% PS-TKA.

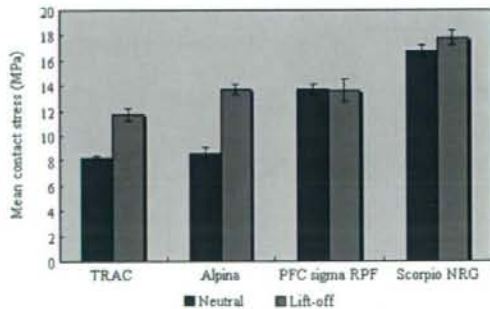


Fig. 10. Mean contact stress (MPa) of each component with neutral and 3 mm lift-off of the femoral component at 120° of flexion.

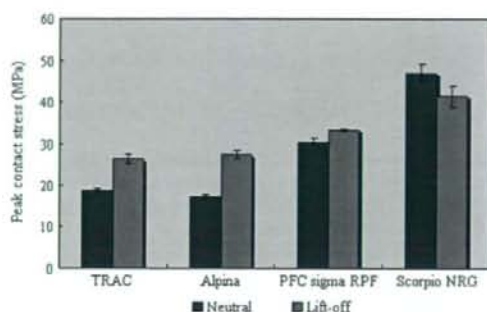


Fig. 11. Peak contact stress (MPa) of each component with neutral and 3 mm lift-off of the femoral component at 120° of flexion.

The maximum value for lift-off was 2.7 mm at 90° flexion. Argenson et al [23] also performed a kinematic analysis of 20 patients who achieved an average weight-bearing range of motion of 125° after PS-TKA (LPS Flex; Zimmer, Warsaw, Ind). They reported 40% of patients experienced femoral lift-off, with a maximum value of 2.5 mm at maximum knee flexion. We therefore examined the contact stress of the post-cam interface under the conditions of 3 mm femoral condylar lift-off at 120° flexion in comparison to neutral setting. Our study demonstrated that the TRAC and Alpina units exhibited increased contact stress and decreased contact area with 3 mm of lift-off. Of all of the prostheses, the TRAC and Alpina displayed the greatest increments of contact stress with lift-off. The configuration of the post-cam in these prostheses conformed to a greater extent than the other prostheses in the sagittal plane (Figs. 1 and 2). Therefore, these results indicated that vertical motion of the femoral component, such as that seen during lift-off, might lose conformity at the post-cam interface, resulting in increased contact stress. In contrast, the PFC sigma RPF and Scorpio NRG prostheses did not exhibit remarkable changes in either contact area or stress with lifting up of the femoral component. The post-cams of these units were less constrained in the proximal-distal direction (Figs. 3 and 4). This design feature avoids excessive stresses between the polyethylene insert and the tibial baseplate during lift-off of the femoral component.

One of the limitations of this study is that the tests were performed under static conditions at only 3 angles. It remains possible that the post-cam designs examined in this study may exhibit their highest contact stresses at angles other than 90°, 120°, or 150° of flexion. Studies examining these units under

dynamic conditions are necessary to assess the force distribution of the post-cam mechanism. Another limitation of this study is that only a relatively low force (500 N) [11,15,16] was used; forces applied to the tibiofemoral articular surface were ignored. This force was determined by previous biomechanical studies. Large force would result in high contact stress, but tendency of the data would not change significantly. The prostheses used in this study has 5 to 7 size variations, but the size of the post does not increase as the tibial size goes up in 3 of 4 prostheses (Table 2). We did not completely match the A-P and M-L size of the components, but the second or third smallest size was used. Therefore, we believe, the size difference would minimally affect the results. Three millimeters of lift-off motion was chosen based on kinematic data of previous studies [23,24] because we currently do not have kinematic data of all the prostheses we tested. However, there is the possibility that each of the prostheses might have different lift-off motions. This is another limitation of this study. Regardless of these shortcomings, we believe that this study reveals important information about the post-cam contact mechanism.

In conclusion, recent modifications of the post-cam designs used in PS-TKA have increased the contact area and conformity, which may contribute to a lower contact stress during deep knee flexion. In this study, however, none of the prostheses examined exhibited consistently low contact stresses throughout flexion. In addition, the contact stresses of the post-cam interface increased significantly with femoral condylar lift-off in a number of the prostheses. Further modification of the post-cam mechanism is necessary to provide lower risk for polyethylene failure in the knee with over flexion.

References

1. Insall JN, Hood RW, Flawn LB, et al. The total condylar knee prosthesis in gonarthrosis. A five to nine-year follow-up of the first one hundred consecutive replacements. *J Bone Joint Surg Am* 1983;65:619.
2. Colizza WA, Insall JN, Scuderi GR. The posterior stabilized total knee prosthesis. Assessment of polyethylene damage and osteolysis after a ten-year-minimum follow-up. *J Bone Joint Surg Am* 1995; 77:1713.
3. Rodriguez JA, Bhende H, Ranawat CS. Total condylar knee replacement: a 20-year followup study. *Clin Orthop* 2001;388:10.
4. Callaghan JJ, O'Rourke MR, Goetz DD, et al. Tibial post impingement in posterior-stabilized total knee arthroplasty. *Clin Orthop* 2002;404:83.

5. Chiu YS, Chen WM, Huang CK, et al. Fracture of the polyethylene tibial post in a NexGen posterior-stabilized knee prosthesis. *J Arthroplasty* 2004;19:1045.
6. Mauerhan DR. Fracture of the polyethylene tibial post in a posterior cruciate-substituting total knee arthroplasty mimicking patellar clunk syndrome: a report of 5 cases. *J Arthroplasty* 2003;18:942.
7. Mestha P, Shenava Y, D'Arcy JC. Fracture of the polyethylene tibial post in posterior stabilized (Insall Burstein II) total knee arthroplasty. *J Arthroplasty* 2000;15:814.
8. Mikulak SA, Mahoney OM, dela Rosa MA, et al. Loosening and osteolysis with the press-fit condylar posterior-cruciate-substituting total knee replacement. *J Bone Joint Surg Am* 2001;83-A:398.
9. Puloski SK, McCalden RW, MacDonald SJ, et al. Tibial post wear in posterior stabilized total knee arthroplasty. An unrecognized source of polyethylene debris. *J Bone Joint Surg Am* 2001;83-A:390.
10. Sultan PG, Most E, Schule S, et al. Optimizing flexion after total knee arthroplasty: advances in prosthetic design. *Clin Orthop* 2003;416:167.
11. Dahlkvist NJ, Mayo P, Seedhom BB. Forces during squatting and rising from a deep squat. *Eng Med* 1982;11:69.
12. Li G, Most E, Otterberg E, et al. Biomechanics of posterior-substituting total knee arthroplasty. An in vitro study. *Clin Orthop* 2002;404:214.
13. Li G, Zayontz S, DeFrate LE, et al. Kinematics of the knee at high flexion angles. An in vitro investigation. *J Orthop Res* 2004;19:90.
14. Li G, Zayontz S, Most E, et al. In situ forces of the anterior and posterior cruciate ligaments in high knee flexion: an in vitro investigation. *J Orthop Res* 2004;22:293.
15. Nagura T, Dyrby CO, Alexander EJ, et al. Mechanical loads at the knee joint during deep flexion. *J Orthop Res* 2002;4:881.
16. Wilk KE, Escamilla RF, Fleisig GS, et al. A comparison of tibiofemoral joint forces and electromyographic activity during open and closed kinetic chain exercises. *Am J Sports Med* 1996;24:518.
17. Nakayama K, Matsuda S, Miura H, et al. Contact stress at the post-cam mechanism in posterior-stabilized total knee arthroplasty. *J Bone Joint Surg Br* 2005;87-B:483.
18. D'Lima DD, Hermida JC, Chen PC, et al. Polyethylene wear and variations in knee kinematics. *Clin Orthop Relat Res* 2001;1240:30.
19. Currier JH, Duda JL, Aperling DK, et al. In vitro simulation of contact fatigue damage found in ultrahigh molecular weight polyethylene components of knee prostheses. *Proc Inst Mech Eng* 1998;212:293.
20. Bartel DL, Rawlinson JJ, Burstein AH, et al. Stresses in polyethylene components of contemporary total knee replacements. *Clin Orthop Relat Res* 1995:76.
21. D'Lima DD, Chen PC, Colwell Jr CW. Polyethylene contact stresses, articular congruity, and knee alignment. *Clin Orthop* 2001;392:232.
22. Ishikawa H, Fujiki H, Yasuda K. Contact analysis of ultrahigh molecular weight polyethylene articular plate in artificial knee joint during gait movement. *J Biomech Eng* 1996;118:377.
23. Argenson JNA, Scuderi GR, Komistek RD, et al. In vivo kinematic evaluation and design considerations related to high flexion in total knee arthroplasty. *J Biomech Eng* 1996;118:377.
24. Denis DA, Komistek RD, Walker SA, et al. Femoral condylar lift-off in vivo in total knee arthroplasty. *J Bone Joint Surg Br* 2001;83-B:32.
25. Nilsson KG, Karrholm J. Increased varus-valgus tilting of screw-fixed knee prostheses: stereoradiographic study of uncemented versus cemented tibial components. *J Arthroplasty* 1993;8:529.
26. Wasielewski RC, Galat DD, Komistek RD. An intraoperative pressure-measuring device used in total knee arthroplasties and its kinematics correlations. *Clin Orthop* 2004;427:171.
27. Matsuda S, White SE, Williams II VG, et al. Contact stress analysis in meniscal bearing total knee arthroplasty. *J Arthroplasty* 1998;13:699.
28. Matsuda S, Williams VG, Whiteside LA, et al. A comparison of pressure sensitive film and digital electronic sensors to measure contact area and contact stress. *Orthop Trans* 1995;19:920.
29. Matsuda S, Whiteside LA, White SE. The effect of varus tilt on contact stresses in total knee arthroplasty: a biomechanical study. *Orthopedics* 1999;22:303.
30. Takeuchi T, Lathi VK, Khan AM, et al. Patellofemoral contact pressures exceed the compressive yield strength of UHMWPE in total knee arthroplasties. *J Arthroplasty* 1995;10:363.
31. Buechel FF, Pappas MJ, Makris G. Evaluation of contact stress in metal-backed patellar replacements. A predictor of survivorship. *Clin Orthop Relat Res* 1991:190.
32. Deng M, Latour RA, Ogale AA, et al. Study of creep behavior of ultra-high-molecular-weight polyethylene systems. *J Biomed Mater Res* 1998;40:214.
33. Murantoglu OK, Perinchieff RS, Bragdon CR, et al. Metrology to quantify wear and creep of polyethylene tibial knee inserts. *Clin Orthop* 2003;410:155.
34. Miura H, Higaki H, Nakanishi Y, et al. Prediction of total knee arthroplasty polyethylene wear using the wear index. *J Arthroplasty* 2002;17:760.

Evaluation of impingement of the anterior tibial post during gait in a posteriorly-stabilised total knee replacement

S. Hamai,
H. Miura,
H. Higaki,
T. Shimoto,
S. Matsuda,
Y. Iwamoto

From Kyushu
University, Fukuoka,
Japan

Mechanical failure because of wear or fracture of the polyethylene tibial post in posteriorly-stabilised total knee replacements has been extensively described. In this study of 12 patients with a clinically and radiologically successful NexGen LPS posteriorly-stabilised prosthesis impingement of the anterior tibial post was evaluated in vivo in three dimensions during gait using radiologically-based image-matching techniques.

Impingement was observed in all images of the patients during the stance phase, although the NexGen LPS was designed to accommodate 14° of hyperextension of the component before impingement occurred. Impingement arises as a result of posterior translation of the femur during the stance phase. Further attention must therefore be given to the configuration of the anterior portion of the femoral component and the polyethylene post when designing posteriorly-stabilised total knee replacements.

Kinematic analysis of many designs of total knee replacement (TKR) with subjects performing various functional activities is now available.¹⁻⁸ Most of these fluoroscopic studies have focused on the movement of the femoral component relative to the tibial tray. There is very little information about the relative movement between the femoral component and the polyethylene tibial insert, especially regarding impingement of the anterior post. Patients with a TKR may extend their knees during gait,⁹ with contact of the anterior tibial post.¹⁰

Flexion of the femoral component and/or the posterior tibial slope allow impingement of the femoral cam on the anterior aspect of the tibial post.⁹⁻¹³ However, in many cases with severe wear or fracture of the tibial post, no specific malposition or malalignment of either the femoral or the tibial components could be identified.¹³⁻¹⁵ Without relative hyperextension of the implant, posterior translation of the femur relative to the tibia could result in impingement against the anterior post. The position of the femur relative to the tibia near full extension is determined by the surface geometry of the articular components, the cam-post mechanism, and the quadriceps force under weight-bearing conditions.¹⁶ The tibial post may function as a substitute for the anterior cruciate ligament (ACL) by providing anterior stability of the knee in low degrees of flexion.

The main purpose of this study was to determine whether the intercondylar notch of the femoral component impinges on the anterior aspect of the tibial post during gait with a posteriorly-stabilised TKR using high-resolution dynamic flat-panel detector images. The secondary purpose was to observe whether there was a correlation between the sagittal alignment of knee prostheses and the impingement on the anterior post under dynamic weight-bearing conditions.

Patients and Methods

A total of 12 patients who had a good outcome following TKR were included in the study following informed consent and approval from the institutional review board. There were two men and ten women with a mean age of 73 years (67 to 86). Their mean height was 149 cm (137 to 157) and their mean weight was 62 kg (45 to 71). The mean pre-operative extension of the knee was -10° (-25° to 0°) and the mean pre-operative flexion was 110° (25° to 130°). The pre-operative diagnosis was osteoarthritis in seven knees and rheumatoid arthritis in five. All the patients received a posteriorly-stabilised TKR (NexGen LPS, Zimmer Inc., Warsaw, Indiana). According to the manufacturer, this implant is designed to avoid impingement of the anterior post in up to 14° of hyperextension without anteroposterior movement of the femoral component. The spine-cam mechanism is designed to work for knee flexion

■ S. Hamai, MD, PhD, Orthopaedic Surgeon
 ■ H. Miura, MD, PhD, Orthopaedic Surgeon, Associate Professor
 ■ S. Matsuda, MD, PhD, Orthopaedic Surgeon, Assistant Professor
 ■ Y. Iwamoto, MD, PhD, Orthopaedic Surgeon, Professor and Chairman Department of Orthopaedic Surgery Graduate School of Medical Sciences, Kyushu University, 3-1-1 Maidashi, Higashi-ku, Fukuoka 812-8582, Japan.

■ H. Higaki, PhD, Mechanical Engineer, Professor
 ■ T. Shimoto, PhD, Mechanical Engineer Department of Mechanical Engineering Faculty of Engineering, Kyushu Sangyo University, 2-3-1 Matsugadai, Higashi-ku, Fukuoka 813-8503, Japan.

Correspondence should be sent to Associate Professor H. Miura; e-mail: miura@ortho.med.kyushu-u.ac.jp

©2008 British Editorial Society of Bone and Joint Surgery doi:10.1302/0301-620X.90B9.20298 \$2.00

J Bone Joint Surg [Br]
 2008;90-B:1180-5.
 Received 5 October 2007;
 Accepted after revision 24 April 2008



Fig. 1a



Fig. 1b

Gait was analysed a) on a treadmill at 0.8 m/s while b) movement of the knee was observed using a large flat-panel radiological image detector.

angles above 75°, providing stability in the sagittal plane and also allowing for posterior rollback in flexion to substitute for the posterior cruciate ligament.

The mean follow-up was for 19 months (4 to 49), the mean post-operative extension was -3° (-10° to 0°) and the mean post-operative flexion was 117° (55° to 135°). The mean knee score based on the Knee Society clinical rating system¹⁷ was 95 (82 to 100) and the functional score was 77 (35 to 100).

Surgical technique. All the operations were performed by the senior author (HM). The components were aligned to allow the mechanical axis to pass through the centre of the prosthetic knee. On the sagittal plane, the femoral bone cut was planned to be perpendicular to the anatomical axis and care was taken to avoid notching the anterior cortex. An 8 mm intramedullary femoral cutting guide was passed into the entry point on the femur, which was pre-determined by anteroposterior and lateral radiographs. The tibial bone cut on the sagittal plane was planned to be parallel to the lateral anatomical tibial slope. The rotational alignment was adjusted to the epicondylar axis and the tibial tuberosity. Soft tissue balancing was performed to achieve varus and valgus stability in both extension and flexion.

Kinematic analysis. Continuous sagittal radiological images of gait on a treadmill at 0.8 m/s were obtained for each patient using a flat-panel detector (Hitachi, Clavis, Tokyo, Japan). This produced 3 frames per second with an image area of 397 mm (H) × 298 mm (V), and 0.20 mm × 0.20 mm/pixel resolution (Fig. 1). The higher contrast resolution of the radiological images provided the basis for an even greater improvement in accuracy.^{18,19} The flat-panel detector was useful in capturing dynamic activities because

of its broader outlook than fluoroscopy. Three images of single-leg stance and three of the swing phase were captured from different gait cycles and analysed using an image-matching technique.²⁰ A total of 72 images were used for the analysis: 36 for each of the swing and stance phase.

The angles of flexion and axial rotation of the components were measured using the image-matching method.²⁰ The positive or negative values of flexion were defined as flexion or extension of the femoral relative to the tibial component. The positive or negative values of rotation were defined as the internal or external rotation of the femoral relative to the tibial component. Impingement of the anterior post was determined by the intersection of the 3D computer-aided design (CAD) model surfaces of the femoral component and the tibial polyethylene insert. This was obtained by using the CAD program (SolidWorks 2001Plus SP3.0, SolidWorks Corporation, Concord, Massachusetts) (Fig. 2). The minimum distance between the femoral trochlea and the anterior aspect of the tibial post was also measured in the mid-sagittal plane of the tibial insert (Fig. 3). The positive or negative value of the minimum distance was defined as the anterior or posterior position of the femoral trochlea relative to the anterior aspect of the tibial post. The skeletal flexion angle between the axes of the femoral and tibial shafts was measured on the sagittal radiological images using an angle scale. A radiological assessment of the flexion angle of the femoral component and the posterior tibial tilt angle on the lateral view was performed according to the Knee Society roentgenographic evaluation.²¹ Post-operative limb alignment in the coronal plane was measured by drawing a mechanical axis on each limb on a full-



Fig. 2a

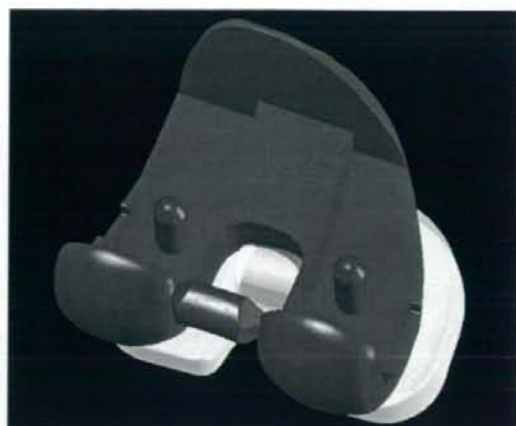


Fig. 2b

Examples of oblique upward views of the 3D computer-aided design models, determined using image-matching techniques. Based on the configuration of the articular surfaces of the femoral component and the polyethylene insert, it was possible to determine whether the femoral trochlea impinged on the anterior aspect of the tibial post in 3D in a) the swing and b) the stance phases of gait.



Fig. 3a



Fig. 3b

The minimum distances between the femoral trochlea and the anterior aspect of the tibial post at the a) the swing and b) the stance phases of gait were determined in the mid-sagittal plane of the tibial insert.

length standing radiograph. The weight-bearing ratio was calculated by measuring the distance from the medial edge of the proximal tibia to the point of intersection with the mechanical axis divided by the entire width of the proximal tibia.^{22,23} A percentage was calculated by multiplying this ratio by 100%. Statistical analysis was per-

formed using a data analysis system (Stat View 5.0, Abacus Concepts Inc., Berkeley, California). The two-factor factorial analysis of variance (ANOVA) and *post hoc* tests (Bonferroni/Dunn) were used to determine the statistical significance at the 95% confidence interval level of the compared results ($p < 0.05$).

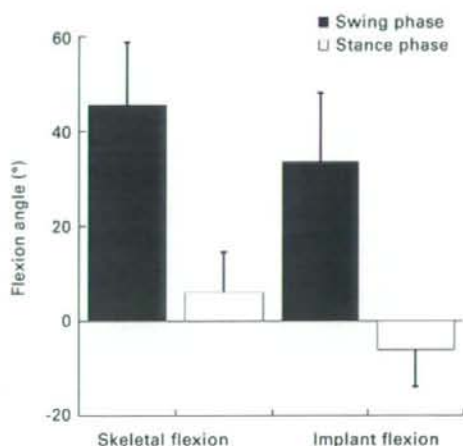


Fig. 4

Bar chart showing the average angles of skeletal and implant flexion at the swing and stance phases of gait.

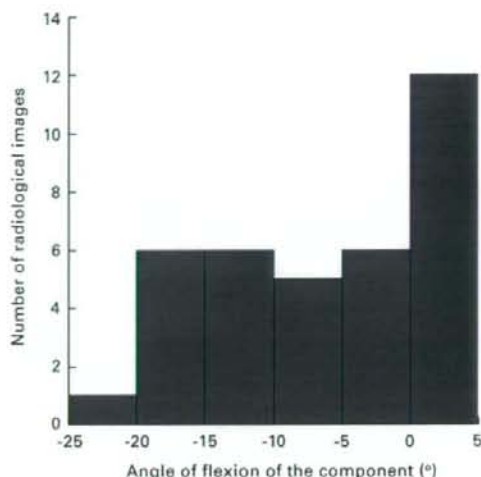


Fig. 5

The distribution of the angle of flexion of the component at the stance phase of gait.

Results

The angles of skeletal flexion and of flexion of the components at the swing/stance phase are shown in Figure 4. At the stance phase, 12 of 36 images represented the flexed position ($\leq 3.5^\circ$), and seven represented hyperextension of more than 15° (Fig. 5). The mean rotation angle at the swing/stance phase was -6.6° (SD 3.5)/ -1.0° (SD 3.0). There was a significant difference in the angles of skeletal flexion ($p < 0.0001$), component flexion ($p < 0.0001$) and axial rotation ($p < 0.0001$) between the stance and swing phases.

Impingement of the anterior post was observed in all the 36 radiological images in 12 knees at the stance phase (Fig. 6). In at the swing phase, all images showed no contact in the anterior or posterior aspects of the tibial post. The mean amount of the minimum distance at the swing/stance phase was 13.4 mm (SD 6.0)/ -0.9 mm (SD 0.8) and this was statistically significant ($p < 0.0001$).

The mean post-operative alignment of the femoral component on the lateral radiograph was 5.6° (SD 2.7) of flexion relative to the distal half of the axis of the femoral shaft. The mean post-operative alignment of the tibial component on the lateral radiograph was 5.9° (SD 2.9) of posterior tilt relative to the proximal half of the axis of the tibial shaft. The mean value of the sagittal alignment of the femoral and tibial components was 11.6° (SD 4.6). The mean post-operative weight-bearing ratio was 52% (SD 10).

Discussion

This study examined impingement of the anterior tibial post of a posteriorly-stabilised TKR during gait using a high-resolution flat-panel radiological detector. All the patients had a successful NexGen posteriorly-stabilised TKR and showed impingement of the anterior tibial post during the stance phase of gait. There was no hyperextension and/or instability on clinical examination in any of the knees. There was no evidence of component malpositioning on radiological analysis of the knees. In the stance phase, the mean skeletal alignment showed low flexion, but the average component alignment was approximately 6° of hyperextension. Even in low component flexion ($\leq 3.5^\circ$), the intercondylar notch of the femoral component impinged on the anterior aspect of the tibial post. During gait, none of the knees flexed into the range of post-cam engagement $> 75^\circ$ flexion in NexGen LPS.

We have demonstrated *in vivo* 3D, impingement of the anterior post during gait in this study. Hyperextension of alignment of the component during the stance phase has been previously described using single-plane fluoroscopy. Banks et al⁹ showed that 41% of knees demonstrated hyperextension during gait, and that the hyperextension of alignment of the component averaged 6° . They noted that the 5° anterior bow and the 5° posterior slope led to approximately 10° of relative hyperextension of the

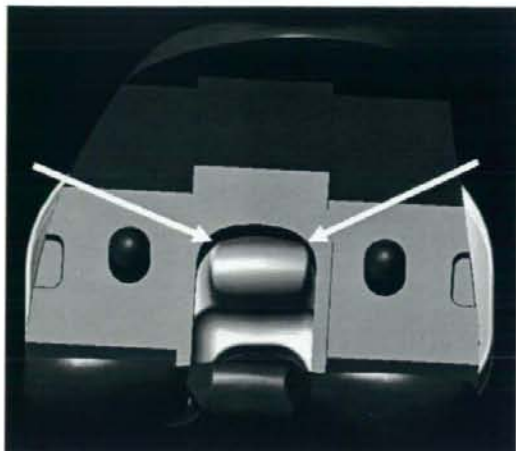


Fig. 6a

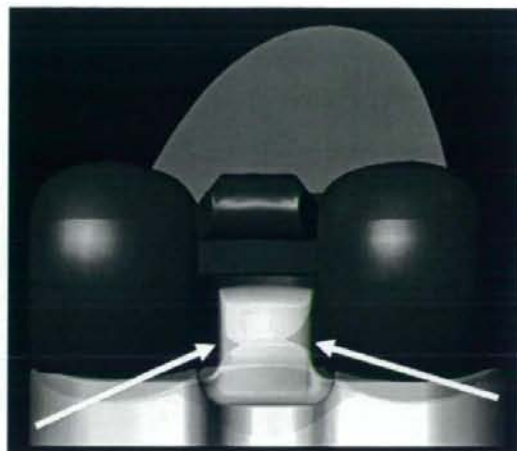


Fig. 6b

Examples of a) top and b) rear views of a patient with a posteriorly stabilised prosthesis experiencing impingement of the anterior post during the stance phase of gait. Viewing from the top, the relatively flat configuration in the anterior aspect of the tibial post compared with the femoral trochlea is seen. White arrows represent the intersections of the 3D model surfaces of the femoral component and the tibial polyethylene insert, which were located on the medial and lateral anterior corners of the tibial post.

component when the knee was in full extension. This is consistent with the findings in our study, which showed that the components were in an average of 12° of hyperextension relative to the sagittal mechanical axis of the knee, because the femoral components were in approximately 6° of flexion and the tibial components had approximately 6° of posterior slope.

Previous studies have indicated that the prevention of impingement of the anterior post depends on the technique of implantation.^{12,13} A flexed femoral component with an inclined tibial component can lead to impingement of the anterior portion of the femoral component on to the tibial post. Although the NexGen LPS was designed to allow for 14° of relative hyperextension of the component without impingement, we found that impingement occurs even without flexion of the femoral component and a posterior tibial slope. The posterior translation of the femur can lead to impingement without hyperextension. Previous studies of posterior cruciate-retaining TKRs using dynamic fluoroscopic analysis revealed that the absence of the ACL caused posterior femoral contact during extension.¹⁻³ During gait, the anteriorly directed shear force on the tibia is normally resisted by the ACL. In the posteriorly stabilised TKR, engagement of the anterior portion of the femoral component on to the tibial post provides a functional substitute for the ACL, resulting in limitation of posterior displacement of the femur relative to the tibia. Stiehl et al⁵ observed that patients having a posterior cruciate-retaining TKR experienced posterior contact positions of both condyles, compared with patients having an anterior and pos-

terior cruciate-retaining TKR. Komistek et al⁶ noted that anterior contact in an anterior cruciate-retaining TKR can be attributed to the presence of the ACL, which resists the anterior tibial shear forces during gait.

In the NexGen LPS, the relatively flat shape of the anterior aspect of the post caused impingement to be located on the medial and the lateral anterior corners of the post. This can lead to excessive stress and wear because of edge loading. This phenomenon has also been seen in previous retrieval studies. Mikulak et al¹⁴ observed that all the 12 retrieved components in their study had evidence of damage to the anterolateral and anteromedial aspects of the post. Haas²⁴ has also noted impingement at the corners of the tibial post in the NexGen LPS. The configuration of the intercondylar notch of the femoral component and the anterior aspect of the tibial post should be designed to provide a larger contact area and prevent edge loading. This may cause chronic wear and fracture of the post, giving a concern as to the long-term prognosis of TKR. The anteroposterior force does not significantly increase during the gait cycle, but repetitive anterior impingement can lead to wear or fracture of the polyethylene post. Recent modifications to provide a larger area of contact have mainly focused on the post-cam mechanism.^{20,25,26} Li et al²⁷ demonstrated that the contact forces in the tibial post increased dramatically as the knee hyperextended, and that the contact force was minimal at 30° of flexion. Surgeons should therefore avoid excessive flexion of the femoral component and posterior slope of the proximal tibial resection.

There are some limitations to this study. Firstly, it did not provide full kinematic analysis of the entire range of move-

ment. It was therefore not possible to observe in which degrees of flexion the intercondylar notch of the femoral component impinged on the anterior aspect of the tibial post. Secondly, the study was limited by the small number of patients. As a result, we could not conclusively state that the cam-post in the NexGen LPS always engaged anteriorly during gait. However, the study did reveal that anterior impingement of the tibial post was a repeatable phenomenon. Finally, the results presented here were obtained using a single type of implant. Further investigations with comparisons of different designs are required.

No benefits in any form have been received or will be received from a commercial party related directly or indirectly to the subject of this article.

References

1. Stiehl JB, Komistek RD, Dennis DA, Paxson RD, Hoff WA. Fluoroscopic analysis of kinematics after posterior-cruciate-retaining knee arthroplasty. *J Bone Joint Surg [Br]* 1995;77-B:884-9.
2. Dennis DA, Komistek RD, Hoff WA, Gabriel SM. In vivo knee kinematics derived using an inverse perspective technique. *Clin Orthop* 1996;331:107-17.
3. Dennis DA, Komistek RD, Colwell CE Jr, et al. In vivo anteroposterior femorotibial translation of total knee arthroplasty: a multicenter analysis. *Clin Orthop* 1998;356:47-57.
4. Banks SA, Markovich GD, Hodge WA. In vivo kinematics of cruciate-retaining and -substituting knee arthroplasties. *J Arthroplasty* 1997;12:297-304.
5. Stiehl JB, Komistek RD, Cloutier JM, Dennis DA. The cruciate ligaments in total knee arthroplasty: a kinematic analysis of 2 total knee arthroplasties. *J Arthroplasty* 2000;15:545-50.
6. Komistek RD, Allain J, Anderson DT, Dennis DA, Goutallier D. In vivo kinematics for subjects with and without an anterior cruciate ligament. *Clin Orthop* 2002;404:315-25.
7. Dennis DA, Komistek RD, Mahfouz MR, Walker SA, Tucker A. A multicenter analysis of axial femorotibial rotation after total knee arthroplasty. *Clin Orthop* 2004;428:180-9.
8. Delport HP, Banks SA, De Schepper J, Bellemans J. A kinematic comparison of fixed- and mobile-bearing knee replacements. *J Bone Joint Surg [Br]* 2006;88-B:1016-21.
9. Banks SA, Harman MK, Hodge WA. Mechanism of anterior impingement damage in total knee arthroplasty. *J Bone Joint Surg [Am]* 2002;84-A(Suppl 2):37-42.
10. Hanson GR, Suggs JF, Kwon YM, Freiberg AA, Li G. In vivo anterior tibial post contact after posterior stabilizing total knee arthroplasty. *J Orthop Res* 2007;25:1447-53.
11. O'Rourke MR, Callaghan JJ, Goetz DD, Sullivan PM, Johnston RC. Osteolysis associated with a cemented modular posterior-cruciate-substituting total knee design: five to eight-year follow-up. *J Bone Joint Surg [Am]* 2002;84-A:1362-71.
12. Callaghan JJ, O'Rourke MR, Goetz DD, et al. Tibial post impingement in posterior-stabilized total knee arthroplasty. *Clin Orthop* 2002;404:83-8.
13. Chiu YS, Chen WM, Huang CK, Chiang CC, Chen TH. Fracture of the polyethylene tibial post in a NexGen posterior-stabilized knee prosthesis. *J Arthroplasty* 2004;19:1045-9.
14. Mikulak SA, Mahoney OM, dela Rosa MA, Schmalzried TP. Loosening and osteolysis with the press-fit condylar posterior-cruciate-substituting total knee replacement. *J Bone Joint Surg [Am]* 2001;83-A:398-403.
15. Hendel D, Garti A, Weisbort M. Fracture of the central polyethylene tibial spine in posterior stabilized total knee arthroplasty. *J Arthroplasty* 2003;18:672-4.
16. Victor J, Bellemans J. Physiologic kinematics as a concept for better flexion in TKA. *Clin Orthop* 2006;452:53-8.
17. Insall JN, Dorr LD, Scott RD, Scott WN. Rationale of the Knee Society clinical rating system. *Clin Orthop* 1989;248:13-14.
18. Fukuoaka Y, Hoshino A, Ishida A. A simple radiographic measurement method for polyethylene wear in total knee arthroplasty. *IEEE Trans Rehabil Eng* 1999;7:228-33.
19. Garling EH, Kaptein BL, Geleijns K, Nelissen RG, Valstar ER. Marker configuration model-based roentgen fluoroscopic analysis. *J Biomech* 2005;38:893-901.
20. Hamai S, Miura H, Higaki H, et al. Kinematic analysis of kneeling in cruciate-retaining and posterior-stabilized total knee arthroplasties. *J Orthop Res* 2008;26:435-42.
21. Ewald FC. The Knee Society total knee arthroplasty roentgenographic evaluation and scoring system. *Clin Orthop* 1989;248:9-12.
22. Andrews M, Noyes FR, Hewett TE, Andriacchi TP. Lower limb alignment and foot angle are related to stance phase knee adduction in normal subjects: a critical analysis of the reliability of gait analysis data. *J Orthop Res* 1996;14:289-95.
23. Matsuda S, Miura H, Nagamine R, et al. Changes in knee alignment after total knee arthroplasty. *J Arthroplasty* 1999;14:566-70.
24. Haas BD. Tibial post impingement in posterior-stabilized total knee arthroplasty. *Orthopedics* 2006;29(9 Suppl):83-5.
25. Nakayama K, Matsuda S, Miura H, et al. Contact stress at the post-cam mechanism in posterior-stabilized total knee arthroplasty. *J Bone Joint Surg [Br]* 2005;87-B:483-8.
26. Huang CH, Lau JJ, Huang CH, Cheng CK. Influence of post-cam design on stresses on posterior-stabilized tibial posts. *Clin Orthop* 2006;450:150-6.
27. Li G, Papannagari R, Most E, et al. Anterior tibial post impingement in a posterior stabilized total knee arthroplasty. *J Orthop Res* 2005;23:536-41.

Kinematic Analysis of Kneeling in Cruciate-Retaining and Posterior-Stabilized Total Knee Arthroplasties

Satoshi Hamai,¹ Hiromasa Miura,¹ Hidehiko Higaki,² Shuichi Matsuda,¹ Takeshi Shimoto,² Kousuke Sasaki,¹ Masaaki Yoshizumi,² Ken Okazaki,¹ Nobuaki Tsukamoto,¹ Yukihide Iwamoto¹

¹Department of Orthopaedic Surgery, Graduate School of Medical Sciences, Kyushu University, 3-1-1 Maidashi, Higashi-ku, Fukuoka 812-8582, Japan

²Department of Mechanical Engineering, Faculty of Engineering, Kyushu Sangyo University, 2-3-1 Matsugadai, Higashi-ku, Fukuoka 813-8583, Japan

Received 17 August 2006; accepted 26 July 2007

Published online in Wiley InterScience (www.interscience.wiley.com). DOI 10.1002/jor.20512

ABSTRACT: Kneeling is an important function of the knee for many activities of daily living. In this study, we evaluated the *in vivo* kinematics of kneeling after total knee arthroplasty (TKA) using radiographic based image-matching techniques. Kneeling from 90 to 120° of knee flexion produced a posterior femoral rollback after both cruciate-retaining and posterior-stabilized TKA. It could be assumed that the posterior cruciate ligament and the post-cam mechanism were functioning. The posterior-stabilized TKA design had contact regions located far posterior on the tibial insert in comparison to the cruciate-retaining TKA. Specifically, the lateral femoral condyle in posterior-stabilized TKA translated to the posterior edge of the tibial surface, although there was no finding of subluxation. After posterior-stabilized TKA, the contact position of the post-cam translated to the posterior medial corner of the post with external rotation of the femoral component. Because edge loading can induce accelerated polyethylene wear, the configuration of the post-cam mechanism should be designed to provide a larger contact area when the femoral component rotates. © 2007 Orthopaedic Research Society. Published by Wiley Periodicals, Inc. *J Orthop Res* 26:435–442, 2008

Keywords: kinematics; kneeling; posterior cruciate ligament; post-cam mechanism; total knee arthroplasty

INTRODUCTION

Kneeling is an important function for many activities of daily living. More than 50% of all patients undergoing total knee arthroplasty (TKA) consider kneeling important and participate in kneeling.¹ Inability to kneel after knee surgery is a frequent cause of dissatisfaction. Kneeling for different functions requires different degrees of knee flexion. Kneeling in 90° of knee flexion has been called "upright kneeling" and kneeling in more than 110° of knee flexion "flexed kneeling."² Flexed kneeling is important especially in Middle and Far Eastern patients as they sit on and rise from the floor. The patella and the tibial tuberosity contact the ground in upright kneeling, while only the tibial tuberosity bears weight in flexed kneeling.³

Kneeling ability depends on many factors. Scar position and skin hypoesthesia can limit kneeling ability. A lateral incision produces less dysesthesia,

fewer neuromas, and less discomfort.⁴ A patient's ability to kneel may be greater than their own perception of their ability to do so.^{2,5} Many patients undergoing TKA avoid kneeling for fear of harming the prosthesis.

Weight-bearing load may be exerted on the patellofemoral articulation and the retained posterior cruciate ligament (PCL) after cruciate-retaining (CR) TKA or the post-cam mechanism after posterior-stabilized (PS) TKA during activities requiring deep flexion.^{6–8} However, very little is known regarding knee kinematics during upright and flexed kneeling, and even less is known about how TKA design affects knee biomechanics at this limit of knee flexion. The purpose of this study was to clarify *in vivo* knee kinematics during kneeling. In addition, we compared kinematics with the joint in a hyperflexed position between CR TKA and PS TKA.

The *in vivo* 3D position and orientation of the components of CR and PS TKA during both upright and flexed kneeling were evaluated using an image-matching method. In a previous study, Komistek et al.⁹ analyzed femorotibial contact positions in static upright kneeling using an iterative computer model-fitting technique. However,

Correspondence to: Hiromasa Miura (Telephone: +81-92-642-5488; Fax: +81-92-642-5507; E-mail: miura@ortho.med.kyushu-u.ac.jp)

© 2007 Orthopaedic Research Society. Published by Wiley Periodicals, Inc.

little information is available on the in vivo dynamic kinematics of kneeling from 90 to 120° of flexion after TKA.¹⁰ In addition, this study analyzed subjects having a PS TKA to determine the contact position at the post-cam mechanism. Nakayama et al.¹¹ measured in vitro contact areas and stresses at the post-cam mechanism using a digital electric stress sensor. However, in vivo post-cam contact positions after PS TKA have not been reported.

We hypothesized that knee flexion angles and type of TKA design would affect the tibiofemoral contact positions during kneeling, and that the post-cam contact position after PS TKA would not be in the center of the post at flexed positions.

MATERIALS AND METHODS

Twenty subjects who had undergone clinically successful TKA and were willing to participate enrolled in the study. Inclusion criteria were the ability to perform both upright and flexed kneeling. All subjects gave informed consent, and an institutional review board approved the study. Ten knees in eight subjects received CR TKA (Foundation knee, Encore Medical Co., Austin, TX) and 10 knees in seven subjects received PS TKA (Nexgen LPS, Zimmer, Inc., Warsaw, IN). The articulating surface geometry of the polyethylene tibial insert is conforming in PS TKA, but relatively flat in CR TKA, allowing femoral rollback produced by tensioning of the PCL during flexion.

The 20 subjects included 18 women and 2 men with an average follow-up of 17.3 months. The preoperative diagnoses were osteoarthritis in 15 knees and rheumatoid arthritis in 5, and the average age at surgery was 71.6 years. Average postoperative knee extension/flexion angle was -2.8/128.4°. The Knee Society score (knee score/function score) was 91.4/80.6. Three experienced surgeons (H.M., S.M., and K.O.) performed all TKAs using a similar standard technique. The components were aligned so that the mechanical axis passed through

the center of the knee prosthesis. Rotational alignment was adjusted to bony landmarks, such as the trans-epicondylar axis and tibial tuberosity. The PCL was retained when it appeared normal in tension and appearance at surgery. Soft tissues were balanced to achieve varus and valgus stability.

Each subject was asked to perform upright and flexed kneeling in maximum knee flexion under radiological surveillance (Fig. 1). Knee flexion in each subject reached more than 120° of knee flexion passively. During kneeling, subjects placed their leg on a box with the ankle joint extended. Continuous X-ray images were taken using a flat panel detector (Clavis, Hitachi, Co., Ltd., Tokyo). The detector provided higher resolution dynamic images (Distortion-free image, 0.20 × 0.20 mm/pixel resolution, three frames/s, with an image area size 397 (H) × 298 (V) mm). The high contrast resolution of X-ray images provided the basis for the required accuracy.^{12,13} Images of kneeling at 90, 100, 110, and 120° of flexion were selected from the continuous images and analyzed using a previously published image-matching technique.^{14,15}

The projected 3D computer-aided design (CAD) models of the femoral and tibial components were superimposed on the 2D radiographic images (Fig. 2a). The 3D CAD models of the components and the tibial insert were reconstructed after 3D shape measurements of the total knee prostheses by a profilometer (Mitsutoyo, Co., Ltd., Kawasaki, Japan) (Fig. 2b). The position of the radiation source relative to the X-ray detector was determined from the projection image of a calibration cage made from an acrylic resin board and metallic balls. Projecting all surface points of the 3D model produced the component silhouette. A model silhouette was matched with the actual silhouette by translating and rotating the 3D CAD model to minimize the number of unmatched pixels between the silhouettes. After the 3D pose of the components was estimated, the 6 degrees of freedom of the femoral component relative to the tibial component were determined by transforming the coordinate systems into one common system.

The accuracy and precision of the measurement technique was determined by in vitro investigations.^{15,16}

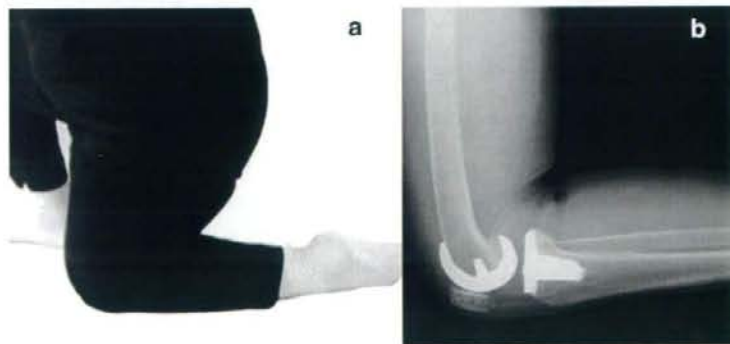


Figure 1. Each subject was asked to perform kneeling from 90° to maximum knee flexion (a). Continuous X-ray images of kneeling were taken using a flat panel detector (b).

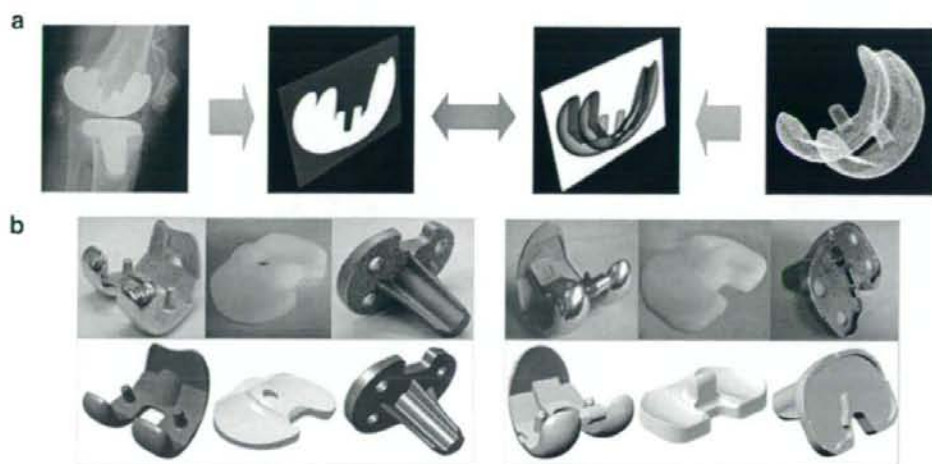


Figure 2. A model silhouette was matched with the actual object silhouette by translating and rotating the 3D CAD models (a). The models of the components (lower stand) were reconstructed at CR TKA (left) and PS TKA (right) after 3D shape measurements of the total knee prostheses (upper stand) by a profilometer (b).

The components mounted on a stage were rotated and translated to known values. The image-matching process was performed for the radiographic images at each position to determine the relative pose of the components. The root-mean-square (RMS) accuracy errors for this process for the femoral component were 0.29 mm for in-plane translation, 0.37 mm for out-of-plane translation, and 0.27° for rotation, and the accuracies for the tibial component were 0.23 mm for in-plane translation, 0.30 mm for out-of-plane translation, and 0.25° for rotation. The maximum errors associated with tracking the position of the tibia relative to the femur were the sum of the RMS errors, which were 0.52, 0.67 mm, and 0.52° respectively, for in-plane and out-of-plane translations and rotation.

The contact positions between the femoral component and tibial insert and tibiofemoral axial rotation were evaluated after both CR and PS TKA (Fig. 3). The contact positions were evaluated by measuring the centroid of contact area between the surfaces of the femoral condyles and the insert using a CAD software program (SolidWorks® 2001Plus SP3.0, SolidWorks Corporation, Concord, MA) (Fig. 3a). If surface separation was recognized, the location of closest proximity between the surfaces of the femoral condyles and the insert was measured in 3D space. The positive or negative value of AP tibiofemoral contact position was defined as anterior or posterior to the midline of the polyethylene insert. The tibiofemoral rotation was evaluated to measure the rotation angle of the femoral component relative to the tibial component (Fig. 3b). The positive or negative value of tibiofemoral rotation was defined as internal or external rotation of the femur relative to tibia. After PS TKA, the medial-lateral and upper-lower translation of contact position

between the femoral cam and tibial post was evaluated (Fig. 3c). The positive or negative value of ML post-cam contact position was defined as medial or lateral to the center of the post. The positive or negative value of proximal-distal post-cam contact position was defined as proximal or distal to the most inferior point of the articular surface.

Statistical analyses were done using Stat View 5.0 (Abacus Concepts, Inc., Berkeley, CA). All values were expressed as the mean \pm standard deviation. The unpaired *t*-test was used to analyze postoperative knee extension/flexion angles and the Knee Society scores (knee score/function score) comparing CR with PS TKA. Two-way, repeated measures ANOVA were used to analyze the tibiofemoral contact positions and tibiofemoral rotations when investigating the effects of knee flexion angle and TKA design and a comparison of the interaction between these two values. Post hoc tests (Bonferroni/Dunn) were used to identify the source of any differences for relevant comparisons. The paired *t*-test was used to analyze the ML post-cam contact position when comparing 90° with 120° of flexion. A value of $p < 0.05$ was considered significant.

RESULTS

The average postoperative extension/flexion angle was $-3.8 \pm 2.5^\circ/129.3 \pm 5.4^\circ$ after CR TKA and $-2.0 \pm 3.3^\circ/127.7 \pm 8.6^\circ$ after PS TKA. No significant differences were found in postoperative knee extension ($p = 0.24$) and flexion ($p = 0.66$) between CR TKA and PS TKA. The Knee Society score (knee score/function score) was $90 \pm 6.3/78 \pm 11.6$

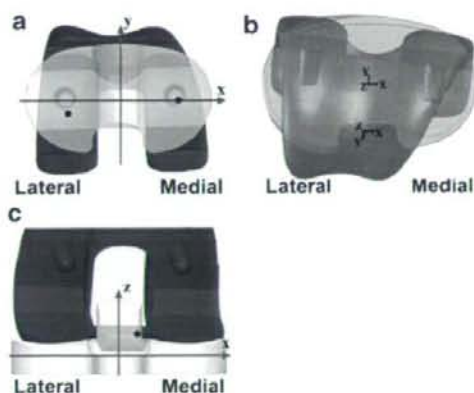


Figure 3. (a) Locations of closest proximity or contact between the femoral component and the tibial insert on the medial and lateral sides. The positive or negative value of the AP tibiofemoral contact position was defined as anterior or posterior to the midline of the tibial insert. (b) The rotation angle of the femoral component relative to the tibial component. The positive or negative value of tibiofemoral rotation was defined as internal or external rotation of the femur relative to tibia. (c) Location of contact between the femoral cam and tibial post after PS TKA. The positive or negative value of medial-lateral post-cam contact position was defined as medial or lateral to the center of the post. The positive or negative value of proximal-distal post-cam contact was defined as proximal or distal to the most inferior point of the articular surface.

for CR and $93 \pm 5.7/82 \pm 13.8$ for PS TKA. No significant differences (knee score: $p = 0.27$; function score: $p = 0.59$) were found between CR TKA and PS TKA.

The average AP tibiofemoral contact positions in 90° of flexion after PS TKA were significantly ($p < 0.0001$) more posterior than after CR TKA with both condyles (Table 1 and Fig. 4). Kneeling from 90 to 120° of flexion produced a posterior femoral rollback for both designs. Anterior femoral translation was not found for any subject from 90 to 120° of flexion. A significant interaction was found between flexion position and TKA design (ANOVA, $p < 0.01$), indicating that the pattern of changes during kneeling differed between TKA designs. The total rollback after PS TKA (medial = -5.2 ± 2.4 mm, range -1.1 to -8.5 mm; lateral = -4.8 ± 3.2 mm, range -0.3 to -10.1 mm) was more than after CR TKA (medial = -4.3 ± 3.7 mm, range -0.1 to -11.4 mm; lateral = -2.4 ± 1.4 mm, range -0.3 to -4.4 mm) with both condyles. The average AP tibiofemoral contact positions in 120° of flexion after PS TKA were significantly ($p < 0.0001$) more posterior than after CR TKA with both condyles (Table 1).

Changes in the rotation angle from 90 to 120° of flexion were $0.4 \pm 2.5^\circ$ (range -2.8 to 4.4°) after CR TKA and $-1.3 \pm 0.8^\circ$ (range -2.3 to -0.1°) after PS TKA. After PS TKA, the change in the external rotation was consistently recognized in each 10° of flexion. The rotation angle in 120° of flexion was $-7.5 \pm 5.4^\circ$ (range -15.7 to -0.5°) after CR TKA and $-6.9 \pm 4.1^\circ$ (range -12.9 to -2.1°) at PS TKA. The femoral components for both designs continued to show external rotation from 90° to 120° of flexion. More than 10° of the external rotation was recognized during kneeling for both designs (CR, 4; PS, 3).

The average ML post-cam contact position in 90° of flexion was 4.0 ± 2.2 mm (range 0.1 to 6.1 mm) medial from the center of the post with external rotation of the femoral component (Table 1 and Fig. 4c). 1.2 ± 1.2 mm (range 0.1 to 3.4 mm) medial translation of the post-cam contact position occurred from 90 to 120° of flexion because the femoral component rotated externally. The average ML post-cam contact position in 120° of flexion was significantly more medial than in 90° ($p < 0.05$). The average proximal-distal post-cam contact position in 90° of flexion was proximal from the most inferior point of the articular surface (Table 1 and Fig. 4c). 1.4 ± 0.9 mm (range 0.0 to 2.4 mm) distal translation of the post-cam contact position occurred from 90 to 120° of flexion. No proximal translation was observed from 90 to 120° of knee flexion.

DISCUSSION

Kneeling in more than 110° of knee flexion tends to produce posterior translation of the tibia relative to the femur because the tibial tuberosity bears weight.² The ground reaction force on the tibial tuberosity causes a posterior directed shear force on the tibia during kneeling. However, posterior translation is prevented by the retained PCL after CR TKA and the post-cam mechanism after PS TKA. Without PCL retention or the post-cam mechanism, the femoral component would not rollback posteriorly, instead translating anteriorly. If the retained PCL and the post-cam mechanism did not provide posterior rollback, an excessive patellofemoral contact force may occur. In this study, kneeling from 90 to 120° of flexion produced posterior rollback in both designs (Fig. 4a and b). Previous studies reported that the retained PCL after CR TKA reproduces posterior rollback.¹⁷⁻²⁰ In addition, after PS TKA, the post-cam mechanism was designed to function over 75° of knee flexion, so we can assume

Table 1. AP Tibiofemoral Contact Positions [+ Anterior, - Posterior] and Tibiofemoral Rotation [+ IR, - ER] after Both CR and PS TKA, and the ML [+ Medial, - Lateral] and Proximal-Distal [+ Proximal from the Most Inferior Point of the Articular Surface] Post-cam Contact Position after PS TKA while Kneeling from 90° to 120° of Knee Flexion

AP Tibiofemoral Contact Positions (mm)		
Cruciate-retaining TKA	Medial Condyle/Lateral Condyle	Rotation (°)
90°	4.2 ± 3.6 ^a /-4.8 ± 3.3 ^a	-7.8 ± 4.8
100°	2.6 ± 2.5 ^a /-5.4 ± 3.4 ^a	-7.6 ± 4.7
110°	1.1 ± 2.8 ^a /-6.1 ± 3.4 ^a	-7.5 ± 5.3
120°	-0.1 ± 3.3 ^a /-7.2 ± 3.9 ^a	-7.5 ± 5.4
ML Tibiofemoral Contact Positions (mm)		
Posterior-stabilized TKA	Medial Condyle/Lateral Condyle	Rotation (°)
90°	-3.7 ± 3.2 ^a /-10.5 ± 3.3 ^a	-5.6 ± 4.2
100°	-5.8 ± 4.1 ^a /-12.2 ± 1.9 ^a	-5.9 ± 4.2
110°	-7.6 ± 4.1 ^a /-14.3 ± 1.2 ^a	-6.4 ± 4.1
120°	-8.9 ± 4.6 ^a /-15.3 ± 2.1 ^a	-6.9 ± 4.1
Post-cam Contact Position (mm)		
Posterior-stabilized TKA	Medial-lateral/Proximal-distal	
90°	4.0 ± 2.2/7.6 ± 0.7	
100°	4.3 ± 2.3/6.9 ± 0.5	
110°	4.7 ± 1.5/6.3 ± 0.7	
120°	5.1 ± 1.2/6.2 ± 0.8	

Values are mean ± standard deviation.

^aSignificantly different between CR TKA and PS TKA ($p < 0.05$).

that both the retained PCL and the post-cam mechanism were functioning.

Posterior femoral rollback was preferable to decrease patellofemoral contact force during kneeling. Increased femoral rollback in flexion correlates with reduced patellofemoral contact load in TKA.²¹ This reduction in contact force is attributed to the increased extensor moment arm. Browne et al.²² reported that the design with the longer extensor moment arm required less quadriceps force and reduced patellofemoral compressive force. In PS TKA, contact positions at 90° of flexion were more posterior, and rollback distance with both condyles was longer compared to CR TKA. PS TKA may be preferable to CR TKA to reduce patellofemoral forces during kneeling. Komistek et al.⁹ found similar results using in vivo fluoroscopy to evaluate femorotibial contact positions in upright kneeling, reporting that the PCL has less resistance to the

anterior thrust of the femur relative to the tibia in PS TKA.

The PS design had contact regions located more posterior on the tibial insert in comparison to the CR design. Specifically, the lateral femoral condyle in the PS translated to the posterior edge of the tibial surface during kneeling, although subluxation did not occur. This finding has important implications regarding the location and severity of the polyethylene wear. The posteromedial corner of the lateral compartment of the tibial insert suffered edge loading by combining posterior translation and external rotation of the femoral component during kneeling. Wasielewski et al.²³ and Harman et al.²⁴ showed wear patterns on retrieved polyethylene insert consistent with these articular contact patterns. The contact locations between the femoral component and polyethylene insert during dynamic activities are thus considered to

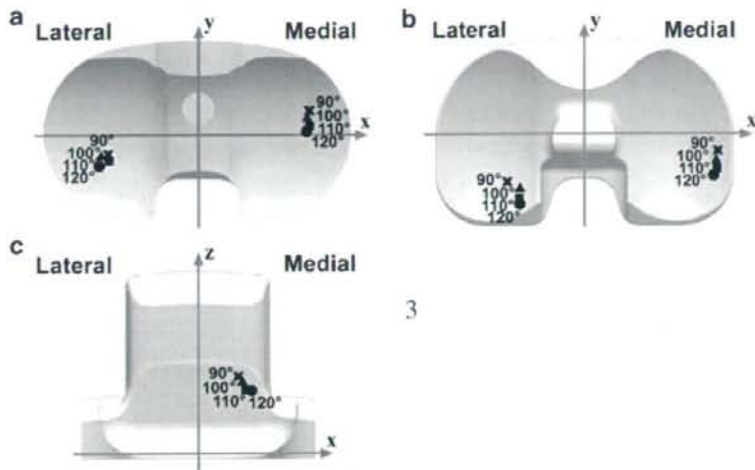


Figure 4. The average tibiofemoral contact positions after CR TKA (a) and PS TKA (b) demonstrated posterior roll back during kneeling from 90 to 120° of knee flexion. The average post-cam contact position after PS TKA translated medially and downward during kneeling (c).

correspond to the wear pattern on the polyethylene articular surface.

No *in vivo* studies have yet focused on the post-cam contact positions in PS TKA. The post-cam contact position during kneeling translated medially and distally along the post (Fig. 4c). The effect of femoral rotation is important for the ML post-cam contact position. External rotation of the femoral component from 90 to 120° of flexion created a medial translation of the post-cam contact position (Fig. 5). Furthermore, 3 of 10 knees after PS TKA had more than 10° of femoral external rotation during kneeling with the risk that the posterior medial corner of the flat-surfaced post could suffer excessive stress because of edge loading. Nakayama et al.¹¹ reported that when the tibial component was rotated 10°, post-cam contact stress increased more than twofold in comparison to neutral rotation. Edge loading may cause chronic wear and fracture of the post, affecting the long-term prognosis following TKA. The post-cam design should be modified to provide a larger contact area and prevent increased contact stress when the femoral component rotates.

Distal translation of the post-cam contact position was found during kneeling. Condylar liftoff is an important issue for proximal–distal post-cam contact position. However, the proximal–distal post-cam contact position demonstrated no proximal translation. The distal translation is more beneficial in preventing posterior dislocation of the tibial component and in decreasing the risk of

fracture of the post. If flexion instability exists after PS TKA, posterior dislocation of the tibial component may occur.^{25–28} However, none of the subjects in this study had evidence of ligamentous laxity or pain on physical examination.

We are concerned about the effect of the load that is exerted on the post-cam mechanism during kneeling. Fracture or polyethylene wear of the post and dislocation of the knee have been reported after PS TKA.^{25–33} In addition, the post-cam mechanism could transmit anteroposterior shear and tensile stresses to the bone–implant interfaces and cause component loosening. After CR TKA, the PCL would play a role in dissipating shear and tensile stresses on the bone–implant interfaces.³⁴ However, further

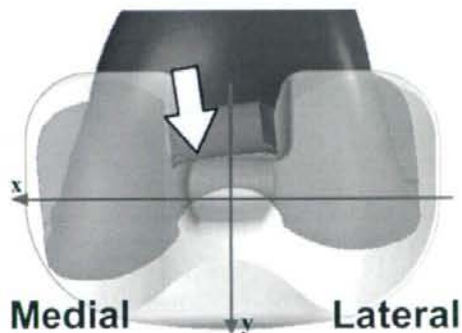


Figure 5. The contact position of the post-cam translated to the posterior medial corner of the post with the external rotation of the femoral component (arrow).